JOURNAL OF PHYSICAL ORGANIC CHEMISTRY, VOL. 5, 382–394 (1992)

MOLECULAR MECHANICS OF BRIDGED FERROCENE DERIVATIVES: CONFORMATIONAL ENERGY SURFACES OF [3]-, [4]- AND [4$_5$] FERROCENOPHANES

JERZY M. RUDZIŃSKI* AND EIJI ŌSAWA†

Department of Knowledge-Based Information Engineering, Toyohashi University of Technology, Tempaku-cho, Toyohashi 441, and Department of Chemistry, Faculty of Science, Hokkaido University, Sapporo 060, Japan

A molecular mechanical model is presented which allows computational interpretation of stereodynamics in ferrocenophanes by using a simple form of bending potential for angles involving the central iron atom and extended to carbon atoms of different cyclopentadienyl rings. Potential energy surfaces of [3]-, [4]- and [4$_5$]ferrocenophanes were studied in detail. For [3]ferrocenophane, the calculated energy barrier of the bridge reversal process agrees well with the experimental value. The previous interpretation of a rigid bridge in [4]ferrocenophane is questioned on the basis of the calculated low barriers. The predominance of experimentally indistinguishable enantiomeric pairs may be responsible for the misinterpretation. [4$_5$]Ferrocenophane is estimated to interconvert into D_5-symmetric global energy minima over barriers of 13–15 kcal mol^{-1} through one-by-one flipping of five tetramethylene bridges.

INTRODUCTION

Bridged ferrocenes have been one of the favourite subjects in organic synthesis, starting with the discovery of ferrocene (**1**)[1–3] and culminating in the recent synthesis of [4]superferrocenophane, the completely tetramethylene-bridged [4$_5$](1,2,3,4,5)ferrocenophane (**2**).[4] With the progress in synthetic strategies to prepare multi-bridged ferrocenes,[5] research on highly strained and symmetrical ferrocenophanes is acquiring greater interest than ever before. One interesting topic relating to the chemistry of ferrocenophanes is their conformational behaviour.

When cyclopentadienyl rings in ferrocene are spanned by a bridge, the latter will impose a restriction on the relative motion of these rings, the severity of which will be determined by steric and conformational demands of the bridge. If the bridging group cannot easily accommodate to the ring–ring separation in ferrocene, the cyclopentadienyl rings suffer tilting, which in turn affects the conformation of the bridge itself. Barr and Watts[6] discussed these problems in their early NMR studies of [N]ferrocenophanes (N = 2–5), and suggested that in monobridged ferrocenophanes the bridging chain undergoes rapid conformational exchange, and that the relative torsional freedom of cyclopentadienyl rings increases with increasing bridge length. The x-ray structure of **2**[4,7] provides other interesting conformational features. As with other known bridged ferrocenes, some averaging process exists in the crystal. A detailed knowledge of these processes can be obtained only by applying computational techniques.[8–13]

We have already reported on a remarkably stable D_5 structure for the hydrocarbon portion of **2** with the tetramethylene bridges in an identical 'zig-zag' conformation by using molecular mechanical calculation.[14] However, further work on the stereodynamics of **2** was suspended at that point since we found none of the known molecular mechanical treatments of ferrocenes to be satisfactory.[15–17]

In some of them, the interactions between iron and cyclopentadienyl rings within the same molecule and also between neighbouring molecules were simply described by the van der Waals-type potentials and electrostatic interactions.[15,18] In other models, 'bonds' were placed between the iron atom and cyclopentadienyl rings, the number of bonds varying from one to five per ring depending on different approximations.[16,17]

In this paper, we describe a new treatment of bridged ferrocenes by molecular mechanics, followed by its

* Present address: Fujitsu Kyushu System Engineering Limited, Hakata Eki Mae 1–5–1, Hakata-ku, Fukuoka 812, Japan.
† Author for correspondence, at Toyohashi.

0894–3230/92/070382–13$11.50

Received 12 February 1992

application to the stereodynamic problems of **2** and a few [*N*]ferrocenophanes. After the completion of this work, a more general approach to transition-metal complexes within an empirical force-field framework has been proposed.[19]

COMPUTATIONAL TECHNIQUES

The program BIGSTRN3[20] was used throughout this work after incorporating the ferrocene force-field parameters described below. Some additional changes were made to cope with the requirements that arose from the ferrocene force field.[21] The reason for choosing BIGSTRN3 is that its capabilities for performing vibrational analysis, force minimization and eigenvector distortion options[22,23] help to identify and correlate stationary points on conformational energy surfaces.

Geometry optimization was performed with the second-derivative Newton–Raphson method. The initial search of stationary points on the conformational energy surfaces was performed by constrained geometry optimization in which dihedral angles chosen as mapping parameters were fixed in a point-by-point fashion. Then, the stationary points of zeroth order (energy minima) were approached by applying unconstrained Newton–Raphson minimization to the conformations obtained.[24] The stationary points of orders higher than zero (one- or multi-dimensional partial maxima) were approached in a similar fashion provided that the starting geometries were very close to the partial maximum. Sometimes, pre-optimization of forces with a variable metric optimizer was required in order to move the points close enough to stationary points which finally could be reached with the Newton–Raphson method. The eigenvector distortion technique[24,25] was always used to correlate saddle points with corresponding energy minima.

Harmonic vibrational frequencies were evaluated for all stationary points found, and were then used to calculate vibrational contributions to the thermodynamic functions. However, the MM2′ force field that we used in this work[26] is not designed for calculating vibrational properties of molecules, and therefore the absolute values evaluated here should be treated with caution.

In presenting conformational potential energy surfaces, the topological approach was used.[27] Topologically reduced surfaces presented in this work are characterized as follows. Two types of critical points[28] are given on a surface, namely energy minima and saddle points. When it was essential to show some would-be paths, multi-dimensional partial maxima are also given. The surfaces were represented by three kinds of graphs, depending on the number of equivalent states drawn for each conformation, representing all diastereoisomeric forms by all their permutational states and correlating them by interconversion paths leads to the 'full' graph. A simpler graph, wherein homomeric species are represented by one point and enantiomeric species by two points, is in most cases sufficient to understand conformational changes of molecules. However, when discussing thermodynamic properties of processes in which differentiation between enantiomers is not important, a much simpler graph suffices ('reduced' graph). On such a graph all homomeric and enantiomeric species of conformations (different diastereoisomeric forms) appear as single points.

BUILDING THE MODEL

We first tested a model in which the bonding interactions between the iron atom and the two cyclopentadienyl rings are approximated by electrostatic attractions in equilibrium with van der Waals repulsions. However, we had to put a large charge on the atoms in order to compensate for the strong repulsions over short (about 2.0 Å) non-bonded iron—carbon distances, and in order to create a reasonable potential of tilting motions of the rings, thus resulting in unreasonably large electrostatic energy contributions to the total steric energy of the system. For this reason, the electrostatic model was abandoned.

In this study we chose a model of the ferrocene molecule in which there are ten bonds between the iron atom and the ten cyclopentadienyl carbon atoms. Interactions involving an iron atom were incorporated in molecular mechanics as follows. An iron atom is bonded to all ten cyclopentadienyl carbon atoms (valence number 10, see Figure 1). Each of the cyclopentadienyl carbon is treated like Allinger's benzene carbon atom,[29] but its valence number is 5, not 4. The extra valency (iron—carbon bond) is hidden when defining valence angles and out-of-plane deformations centred on this carbon atom. In this context, it is still Allinger's aromatic-type carbon. In the same way the Fe—C bonds are hidden when defining the other bond angles and torsion angles in a molecule.

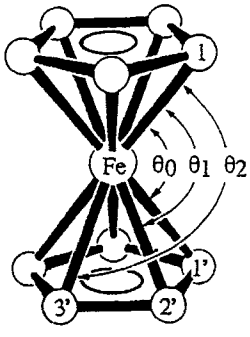

Figure 1. Three sub-types of the C—Fe—C valence angle in ferrocene

Only those bond angles which involve an iron atom and one of each carbon atom belonging to the different cyclopentadienyl rings are explicitly treated as described below. This interaction is important in controlling the tilt motion of the rings in the ferrocene molecule. There are three sub-types of this angle, each having different 'natural' angle values ($\theta_0, \theta_1, \theta_2$, see Figure 1). To cope with the problem of differentiating between these sub-types, which would be very complicated when a molecule is considerably tilted and twisted at the same time, we chose the smallest of the three types of angles as a unique one and ignored the other two. If the C—Fe—C angle is smaller than or equal to the 'natural' angle θ_0, the form of the potential follows Allinger's equation for bending energy.[12] When it is greater than the 'natural' angle, the potential energy is set equal to zero (Figure 2). When a molecule is tilted, some of these angles have θ values greater than θ_0 and there is no force associated with the 'open' angle which would work against this motion, but at the same time some of the C—Fe—C angles are smaller than θ_0 and the force constant associated with this deformation makes up for the deficiency of the force on the opposite site of the ring.

Following the above incorporation, we assigned new atom types for the cyclopentadienyl carbon atoms (atom type 39) and for iron (atom type 40). All but one of the parameters for cyclopentadienyl carbon atoms were transferred from a benzene-type atom (atom type 30). The parameter that was adjusted is the 'natural' length of the C—C bond of a cyclopentadienyl ring. For the new type of Fe—C bond, the force constant (1·40 mdyn Å^{-1}) was adopted from the study of Hyams.[30] The 'natural' Fe—C bond length was designated as adjustable. The van der Waals parameters of iron were also left to be adjusted.

The dipole moment of the Fe—C bond is set here to be 0·29 D based on the following reasoning. Following Pauling's equation (1) for the ionic character of a bond[31] and taking the electronegativities for carbon (2·6) and iron (1·8) atoms from Allred's table,[32] we calculated that the Fe—C bond should be about 14·8% ionic according to equation (1):

$$\text{ionic character} = 1 - \exp[-0{\cdot}25(\chi_A - \chi_B)^2] \quad (1)$$

where χ_A and χ_B are the electronegativities of atoms A and B. Assuming charge distributions of +0·2 on an iron atom and −0·2 on a carbon atom for a fully ionic Fe—C bond, we calculated a bond moment of about 0·29 D for the interatomic separation of 2·040 Å.

The more bridges there are in ferrocenophanes, the more congested the molecule becomes. The non-bonded interactions between hydrocarbon bridges and torsional interactions within the bridge play dominant roles in the equilibrium conformation in such molecules. Since it is more likely that the geometry of the ferrocene moiety in ferrocenophanes is governed by bridges, and since the modified Allinger's molecular mechanics scheme,[33] MM2′,[26] proved good in reproducing geometries and torsional barriers in hydrocarbons, we chose this force field as a basis for the present study.

We used seven ferrocenophane molecules having different numbers of bridges, various lengths and wide range of tilt and twist angles between cyclopentadienyl rings, in addition to ferrocene, to fit the new parameters. The structures of these molecules have been determined by x-ray analysis. They are: ferrocene (**1**),[34] [4$_5$](1,2,3,4,5)ferrocenophane (**2**),[4,7] [3]ferrocenophane (**3**),[35] α,α,α′,α′-tetramethyl[2]ferrocenophane (**4**),[36] [3][3](1,2)ferrocenophane (**5**),[35] [4][3][4](1,2,3)ferrocenophane (**6**),[37] [4](1,1′)[4](3,3′)[3](4,5′)ferrocenophane (**7**)[38] and [4][3][4][3](1,2,3,4)ferrocenophane (**8**).[5] MM2′-optimized geometries of **1**–**8** are shown as ORTEP drawings. Hydrogen atoms are omitted for clarity.

drawings. Hydrogen atoms are omitted for clarity.

Ferrocene parameters were adjusted by minimizing the root-mean-square of errors, which were calculated

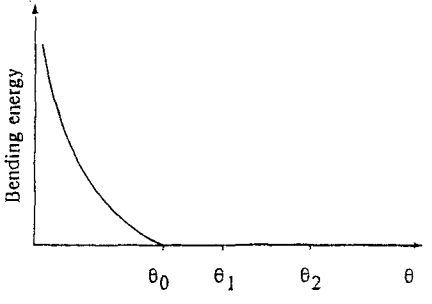

Figure 2. Simplified C—Fe—C bending potential in ferrocene

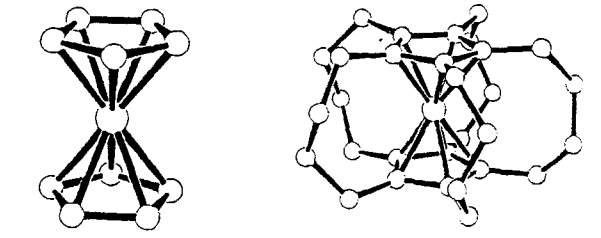

1 2

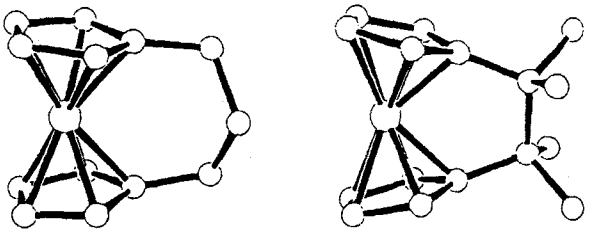

3 4

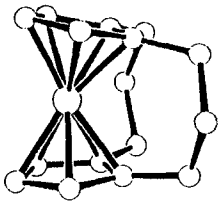

5

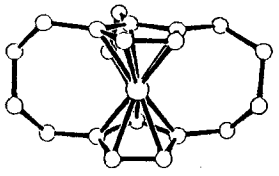

6

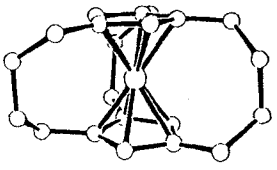

7

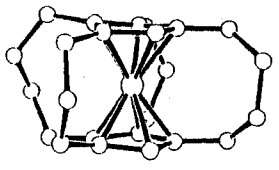

8

over pertinent geometrical features between the MM2′-optimized and experimental structures of **1–8**, and weighted with inverse uncertainties in the experimental measurements:

$$\mathrm{RMS} = \sqrt{\frac{1}{n-1}\sum\left(\frac{\text{error}}{\text{uncertainty}}\right)^2} \qquad (2)$$

When the uncertainties were not reported, appropriate values were assumed. The final set of MM2′ parameters is given in Table 1. Those parameters of the cyclopentadienyl carbon atom (atom type 39) which have been transferred directly from those of the benzene type (atom type 30) are omitted. The optimized parameters are marked with asterisks.

Table 1. MM2′ parameters for ferrocenophanes[a], with atom types 39 = cyclopentadiene carbon atom and 40 = ferrocene-type iron

Stretching:	K_s[b]	L_0[c]
39–39	8·0667	1·428*
39–40	1·4000	2·040*
Non-bonded:	R_{vdW}[d]	ε[e]
40	2·30*	0·20*
Bending:	K_d[f]	θ_0[g]
39–40–39	0·5000*	111·01*
Bond dipole:	μ[h]	
40–39	0·29	

[a] All other parameters involving atom type 39 are the same as those involving the benzene carbon (atom type 30) in MM2′ force field. Asterisks indicate adjusted parameters.
[b] Stretching force constant (mdyn Å^{-1}).
[c] Natural bond length (Å).
[d] Van der Waals radius (Å).
[e] The 'hardness' of an atom (kcal mol^{-1}).
[f] Bending force constant (mdyn Å rad^{-2}).
[g] Natural bond angle (°).
[h] Bond dipole moment (D)

Structural features of ferrocene **1** reported in the literature differ considerably depending on the temperature of the measurements and the methods employed.[34,39–41] For example, the mean C—C bond length of the ring varies from 1·396 to 1·440 Å and the mean C—Fe distance from 2·030 to 2·064 Å.[34,39–41] Those used in the present parameterization were taken from x-ray studies of Seiler and Dunitz[40] for the sake of consistency with the other molecules **2–8**, whose structures came exclusively from x-ray analyses. Our calculated C—C bond length of 1·432 Å and Fe—C distance of 2·039 Å are within the above experimental ranges.

The structure of **3** is taken from the work of Hillman and Austin,[35] and is apparently unreliable. The number of diffraction peaks collected in their measurements was limited by decomposition of the crystal on irradiation with an x-ray beam. Although the uncertainties are large, some values seem unreasonably small. In the same paper, the authors reported the structure of an oxygen analogue of **3**, β-oxa-[3](1,1′)ferrocenophane. The crystal underwent 'not-so-extensive' decomposition and the final structure proved more reliable than **3**. For instance, the C—C bond length of rings in **3** (a bad structure) is 1·380(30) Å but in its oxa analogue (a better structure) it is 1·425(4) Å, which compares well with our calculated value of 1·431 Å. Therefore, we excluded this parameter of **3** from the fitting. Other parameters reported with higher precisions are reproduced well by calculation.

The calculated structural features of **4** agreed well with those measured by Laing and Trueblood.[36] Only one figure is slightly overestimated in our calculations, which is the C_α—$C_{\alpha'}$ bond length [observed 1·584 (14), calculated 1·615 Å]. The strain in **4** is apparent by the fact that the distance of this bridge bond is greater than normal whereas the dihedral angles in the bridge are only about 25°. Other structural features of **4** are also in good agreement with the observed values (C_r—C_α—$C_{\alpha'}$ angle, calculated 109·9°, observed 109·6(2·0)°; Cr—C_α—$C_{\alpha'}$—$C_{r'}$ dihedral angle, calculated 22·1°, observed 25·3°).

The calculated structure of **5** is in nearly perfect agreement with that observed. Since no disorder in the bridge region has been observed, conformation of the bridge should be a good check point for the performance of the force field used. Indeed, calculated dihedral angles along the bridges agree very well with the x-ray values (Cr—Cα—C_β—$C_{\alpha'}$ and C_α—C_β—$C_{\alpha'}$—$C_{r'}$, calculated 65·0°, −65·0°, observed 67·0° ^{av}, −68·0° ^{av}).

The calculated structures of **6**, **7** and **8** are in good agreement with those observed. For ferrocenophanes containing tetramethylene bridges, workers who studied the crystal structures of these compounds often reported disorder in crystals associated with β-carbon atoms of those bridges. In such cases, C_α—C_β and C_β—$C_{\beta'}$ distances from x-ray analyses are too short,

and therefore we have excluded some of these unreliably short bonds in structures **2** and **6–8** from the fitting. The calculated structure of **2** is in line with our previous study of the hydrocarbon part of the molecule.[14]

CONFORMATIONAL ENERGY SURFACES

Before applying the new force field to **2**, we tested its performance by using simpler and experimentally well studied species. Two structures, both having only one bridge spanning the two cyclopentadienyl rings of the ferrocene moiety but with different bridge size, were chosen: [3](1,1)ferrocenophane (**3**) and [4](1,1)ferrocenophane (**9**).

[3](1,1′)ferrocenophane (3)

The x-ray structure of **3**[35] was compared with the MM2′-optimized structure (see above). The bridge in the crystal has a pseudo-chair[42] conformation: the β-atom of the bridge is out of the plane defined by the pair of Cr—C_α bonds. Cyclopentadienyl rings are eclipsed.

The presence of a bridge which spans cyclopentadienyl rings prohibits the nearly free rotation of these rings observed in ferrocene. However, the single bridge does not eliminate liberation along its fivefold axis. The bridge itself can flip and this process is fast on the NMR time scale. The dynamic NMR band shape fitting method has been applied to determine the energy barriers associated with bridge flipping in [3]ferrocenophanes.[42] It showed that the bridge reversal in **3** is closely analogous to the inversion of six-membered ring (the analogy between [3]ferrocenophane and cyclohexane was first recognized by Rosenblum *et al.*[43]). According to Abel *et al.*[42] the molecule interconverts between its two homomeric forms (**3a**, Figure 3), and the transition state with the bridge in an all-*cis* conformation and eclipsed cyclopentadienyl rings (**3c**) has been excluded. The proposed mechanism involves slight rotation about the fivefold axis of the ferrocene unit to a transition-state conformation (**3b**, **3b′**) which in the cyclopentadienyl rings are staggered and the bridge bonds resemble the half-chair conformation of cyclohexane. However, they[42] were not able to conclude whether or not the half-chair conformation is a true transition state. Variable-temperature studies have shown that, at temperatures below $-100\,^{\circ}C$, the bridge reversal process in **3** is slow on the NMR time scale and an energy barrier was evaluated.[44]

Results of the MM2′ calculations are in very good agreement with experimental facts (Figure 3 and Table 2). The global energy minimum structure **3a** has C_s symmetry. The cyclopentadienyl rings are eclipsed and the bridge is in a g^+g^- conformation. This conformation resembles that observed in the crystal, although

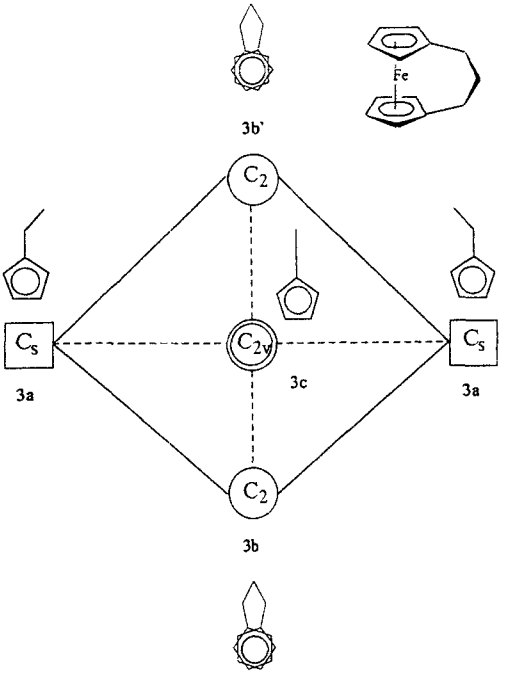

Figure 3. Conformational interconversion graph of [3](1,1′)ferrocenophane (**3**). Squares, circles and a double circle denote minima, saddle points and a two-dimensional partial maximum, respectively. Symmetries of the species are given inside squares and circles. Each stationary point on the surface accompanies a schematic drawing of the conformation. A dashed lines shows the would-be path

dihedral angles along C_α—C_β—$C_{\alpha'}$ bridge bonds differ by about 10° (Table 2). Structure **3a** can interconvert into another permutational isomer via two equivalent saddle points, **3b** and **3b′**, which are enantiomers with C_2 symmetry. The barrier height of this process is calculated to be 9·16 kcal mol^{-1} (1 kcal = 4·184 kJ) on the potential energy scale and 9·45 kcal mol^{-1} on free-energy scale at room temperature. The measured barrier height is 9·66 kcal mol^{-1} (at 206 K) and the corresponding calculated value is 9·14 kcal mol^{-1} (at the same temperature).

The structure **3b** has nearly staggered cyclopentadienyl rings. The relative twist angle of $\pm 28{\cdot}6^{\circ}$ is an amplitude of the motion in the bridge reversal process. A reaction path from one **3a** conformer to another has C_1 symmetry, i.e. the symmetry of the transition vector of **3b** is C_1 symmetric and it corresponds to the symmetry of the imaginary vibration at 143·3i cm^{-1}. During this process bridge dihedral angles, C_r—C_α—C_β—$C_{\alpha'}$ and C_α—C_β—$C_{\alpha'}$—$C_{r'}$, change the sign ($\pm 64{\cdot}8^{\circ}$) through the value of $-22{\cdot}4^{\circ}$ in **3b** (or $22{\cdot}4^{\circ}$ in the process through **3b′**). The difference between the potential energies of **3a** and **3b** comes from

Table 2. Energetic and conformational features of structures corresponding to stationary points found on the MM2′ energy surface of [3](1,1′)ferrocenophane (**3**)

No.	SE[a]	ΔG[b]		ν_{min}[d]	Tilt[e]	Twist[f]	ω[g]	
3a	0·00	0·00	C_s	57·3 (C_1)	9·6	0·0	−64·8	64·8
					(7·6	0·3	−50·0	52·0)[h]
3b	9·16	9·45	C_2	143·3i (C_1)	12·8	−28·6	−22·4	−22·4
		(9·14)[i]		92·2 (C_2)				
3c	12·32	13·44	C_{2v}	287·9i (C_s)	8·6	0·0	0·0	0·0
				63·0i (C_2)				
				159·1 (C_s)				

[a] Relative steric energy (kcal mol^{-1}).
[b] Relative free energy of an enantiomeric pair (kcal mol^{-1}) (T = 298·15 K).
[c] Point group.
[d] Lowest vibrational frequency (cm^{-1}). For saddle points the imaginary frequency (i) is also given. The entries in parentheses denote the symmetry of the vibrational mode.
[e] Tilt angle between ring planes (°).
[f] Relative twist angle of two cyclopentadienyl rings (°).
[g] Dihedral angles, C_r—C_α—C_β—$C_{\alpha'}$ and C_α—C_β—$C_{\alpha'}$—$C_{r'}$ (°).
[h] X-ray values.
[i] Relative free energy of an enantiomeric pair at 206 K.

increased bending (3·7 kcal mol^{-1}) and torsion (4.2 kcal mol^{-1}) interactions in **3b**.

The c_{2v} symmetric structure **3c** with eclipsed cyclopentadienyl rings and a planar bridge has been found to be a two-dimensional partial maximum on the MM2′ energy surface, and is 3·26 kcal mol^{-1} higher in potential energy than the transition state **3b**. This energy difference arises from increased bending and torsion terms. In fact, the ease of twisting along the fivefold axis of the ferrocene unit allows the would-be path involving **3c** as a transition state, which would be the case if the ferrocene moiety of the molecule were rigid, to be avoided.

Hence the suggested mechanism of the bridge reversal[42] is fully supported by our MM2′ conformational energy surface. The calculated barrier height of the bridge reversal differs by only 0·5 kcal mol^{-1} (about 5%) from the measured value.[44] This fact is important because it is the first evidence that the force field parameterized over crystal conformations of ferrocenophanes shows a good performance in the region far from the equilibrium conformations.

[4](1,1′)Ferrocenophane (9)

[4](1,1′)Ferrocenophane (**9**) is the first example of a bridged ferrocene.[45] The preferred conformation of **9** has been the object of numerous studies.[6,20,35,43,46] Although the tetramethylene bridge seems to undergo conformational interconversion, its NMR spectra have not been satisfactorily interpreted,[35] and little is known about the process. Actually, Hillman and Austin[35] classified **9** as a molecule whose bridge does not flip rapidly: its NMR spectrum was described neither as that of a compound with rapidly flipping bridges nor as that of a compound with non-flipping bridges.[35] A crystal of **9** has never been obtained in suitable form for x-ray analysis. The structure of its oxoderivative, namely [4](1,1′)ferrocenophan-6-one (**10**), has been studied by x-ray analysis[47] but was poorly resolved owing to the high thermal motion or disorder. Nonetheless, some information about the preferred conformation of the molecule in the crystal has been obtained, as shown in Table 3, where the structural features are compared with those of the MM2′-calculated global energy minimum conformer of the parent [4](1,1′)ferrocenophane (**9a**). The crystal (orthorhombic, $P2_12_12_1$) is composed of homochiral molecules. It has been concluded that any significant static disorder is unlikely.[47] The tetramethylene bridge appears in a zig-zag conformation and the two cyclopentadienyl rings are almost

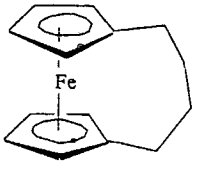

9

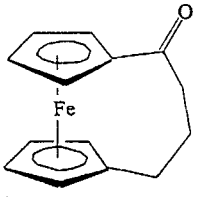

10

Table 3. MM2′-calculated and observed salient structural features of the global energy minimum conformer of [4](1,1′)ferrocenophane (**9a**)[a]

Structural parameter	Calculated	Observed[b]
point group	C_2	$C_1(C_2)$[c]
Tilt	2·5	4·3(1)
Twist	−33·4	−30·5
Ring to ring distance	3·260	3·290 (10)
C_r-C_r distance	1·433	1·407 (12)
C_r-C_α distance	1·499	1·484 (12)
$C_\alpha-C_\beta$ distance	1·538	1·470 (14)
$C_\beta-C_{\beta'}$ distance	1·541	1·484 (13)
$C_r-C_\alpha-C_\beta$ angle	116·9	120·7 (8)
$C_\alpha-C_\beta-C_{\beta'}$ angle	117·3	118·5 (9)
$C_r-C_\alpha-C_\beta-C_{\beta'}$	−79·1	−59·5
$C_\alpha-C_\beta-C_{\beta'}-C_{\alpha'}$	87·6	73·2
$C_\beta-C_{\beta'}-C_{\alpha'}-C_r$	−79·1	−98·0

[a] Distances in Å, angles in degrees. C_r denotes ring carbon atom. Bond lengths and valence angles are averaged.
[b] The observed values correspond to the x-ray structure of [4](1,1′)ferrocenophan-6-one (**10**) of Ref. 46.
[c] The molecule possesses an approximate C_2 axis.

exactly staggered. The tilt angle between the cyclopentadienyl ring planes is 4.3°.

The structural data observed for **10** are consistent with MM2′ calculations on **9a** except for some bond distances and angles which seemed unusual in the crystal but turned out normal by calculation. Structure **9a** is chiral. The two cyclopentadienyl rings are nearly staggered (−33·4°) and the ring planes are nearly parallel (2·5°). The tetramethylene bridge is helical with the $g^-g^+g^-$ arrangement, both end *gauche* angles being identical with respect to the sign and magnitude.

Conformer **9a** can be described as **m–P** and its enantiomeric form **9a′** as **p–M**, where **m** and **p** indicate the negative and positive sign of the twist angle between two cyclopentadienyl rings and **M** and **P** left-handed and right-handed sense of helical bridge, respectively. This designation was used to describe the global energy minimum conformer of [4]superferrocenophane.[14] A search of the energy surface of **9** produced an interconversion graph as shown in Figures 4 (full graph) and 5 (reduced graph). In Figure 4, we use slightly modified indices in order to describe conformational changes of the molecule along the pathway between the global energy minima, **9a** and **9a′**. Thus, let **m–P** be indexed as **m–mpm** and **p–M** as **p–pmp**, where **m** and **p** appearing after the dash means g^- and g^+ arrangements of the dihedral angles along the bridge, respectively. The **x** is used to indicate zero dihedral angle.

Relevant conformational features of the stationary points found on the surface are given in Table 4. The stabilities of three conformers (**9a**, **9c** and **9e**) agree within 1·6 kcal mol^{-1} on both potential and free-energy scales. The highest barrier (**9d**) along the pathway from

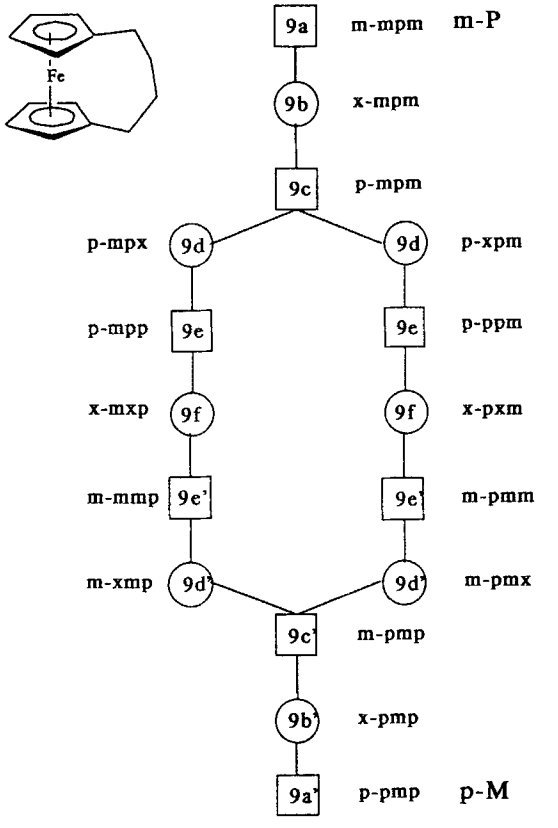

Figure 4. Full graph of the MM2′ conformational energy surface of [4](1,1′)ferrocenophane (**9**). Squares and circles denote minima and saddle points, respectively. Enantiomeric forms of the chiral species are primed. Compare with Figure 5, and see text for the explanation

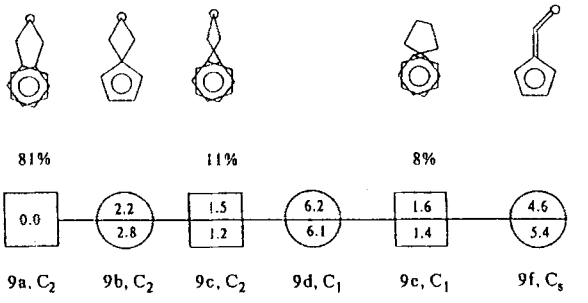

Figure 5. Reduced graph of the MM2′ conformational energy surface of [4](1,1′)ferrocenophane (**9**). Squares and circles denote minima and saddle points, respectively. Relative potential energies (upper entry) and free energies (lower entry) of corresponding conformations are given inside squares and circles. Compare with Table 4. Populations are calculated based on free energies at 298 K

Table 4. Energetic and conformational features of structures corresponding to stationary points found on the MM2′ energy surface of [4](1,1′)ferrocenophane(**9**)

No.	SE[a]	ΔG[b]	PG[c]	ν_{min}[d]	Tilt[e]	Twist[f]	ω[g]
9a	0·0	0·0	C_2	64·9 (C_2)	2·5	−33·4	−79·1
							87·6
							−79·1
9b	2·2	2·8	C_2	43·1i (C_2)	3·3	0·1	−72·7
				136·2 (C_1)			112·7
							−72·7
9c	1·5	1·2	C_2	57·0 (C_2)	1·8	24·0	−62·3
							115·8
							−62·3
9d	6·2	6·1	C_1	176·5i (C_1)	1·3	27·6	−4·1
				60·9 (C_1)			83·9
							−79·0
9e	1·6	1·4	C_1	75·9 (C_1)	3·9	20·2	51·5
							44·0
							−89·7
9f	4·6	5·4	C_s	96·9i (C_1)	3·2	0·0	76·5
				141·8 (C_1)			0·0
							−76·5

[a] Relative steric energy (kcal mol^{-1}).
[b] Relative free energy (kcal mol^{-1}) (T = 298·15 K) (relative to the free energy of an enantiomeric pair of **9a**).
[c] Point group.
[d] Lowest vibrational frequency (cm^{-1}). For saddle points the imaginary frequency (i) is also given. The entries in parentheses denote the symmetry of the vibrational mode.
[e] Tilt angle between ring planes (°).
[f] Relative twist angle of two cyclopentadienyl rings (°).
[g] Dihedral angles along the bridge (°).

9a to **9a′** amounts to 6·1 kcal mol^{-1} (free energy), which is 3·5 kcal mol^{-1} lower than the barrier height in the interconversion of **3**. The twisting motion of the cyclopentadienyl rings in **9** seems extremely easy: the pathway between points **9a** (**m–mpm**) and **9c** (**p–mpm**) (Figures 4 and 5) corresponds to a change of 57·4° in relative twist (from −33·4° to +24·0°) while the conformation of the bridge (**mpm**) remains unchanged. The molecule does not lose its symmetry (C_2) along this pathway and the transition point **9b** (**x–mpm**) is only 2·8 kcal mol^{-1} higher than the global energy minimum **9a**. The twofold degenerate path between the enantiomeric pair **9c** and **9c′** corresponds to the reversal of the bridge itself (**mpm ⇔ pmp**) and it requires nearly twice as much in energy than the twisting motion mentioned above.

The calculated overall energy barrier of the bridge reversal is low and in solution the bridges should flip rapidly. These results contradict Hillman and Austin's interpretation[35] of the NMR spectra of **9**. However, the conformer populations calculated over free energies (T = 298 K, Figure 5) indicate that the experimentally indistinguishable enantiomeric pair **9a** and **9a′** dominates in equilibrium (81%) and maybe this fact is responsible for the observed 'rigidity' of the bridge. The relative ease with which the molecule can twist without changing the bridge conformation can be related to the observed, unusually large temperature factors associated with atoms in one of the rings in the course of x-ray analysis. If the tetramethylene bridge of the molecule in the crystal of **9** does not flip (**mpm ← // → pmp**) and the motion involves only twisting of the cyclopentadienyl rings along the fivefold axis of the ferrocene unit (**m–mpm ↔ x–mpm ↔ p–mpm**), the observed disorder in the crystal of **10** can be understood.

[4$_5$](1,2,3,4,5)Ferrocenophane (2)

The D_5 structure that had previously been proposed as a potential global minimum conformation of [4$_5$](1,2,3,4,5)ferrocenophane (**2**) was confirmed here to be the most stable among several energy minima obtained during the search of its conformational energy surface. This structure (**2a**, and its enantiomer **2a′**, Figure 6) is chiral with six elements of chirality: the ring–ring twist angle, plus (p) or minus (m), and the helical sense of the five tetramethylene bridges, plus (**P**) or minus (**M**). In the case of **2a** the ring–ring twist angle is −8·6°, the three dihedral angles along the five bridges are all in the $g^-g^+g^-$ sequence, hence the direction of helices plus (**P**). Let us designate **2a** as **m–PPPPP** and its enantiomer **2a′** as **p–MMMMM**. The calculated structural parameters of **2a** are nearly

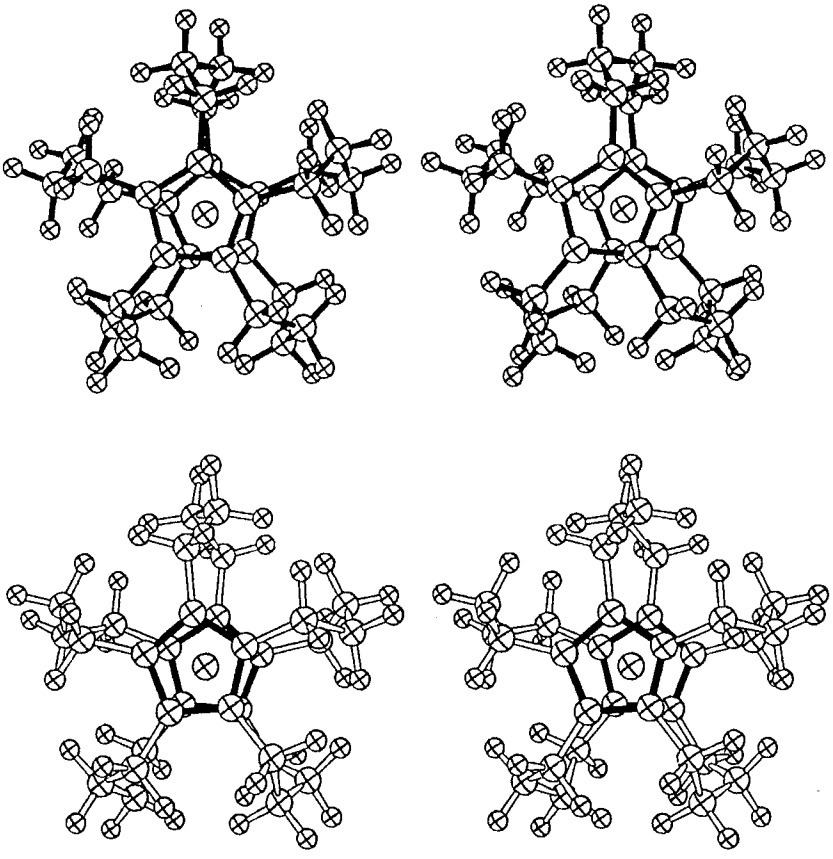

Figure 6. Stereo-drawings of the global energy minimum conformer of [4]superferrocenophane (**2a**) (upper drawing) and its enantiomer (**2a'**) (lower drawing). Black and white colours of the bridges in **2a** and **2a'** denote **P** and **M** helicity, respectively

the same as those of the hydrocarbon portion of [4]superferrocenophane reported in the preliminary study.[14]

The question concerning the nature of disorder in the crystal of **2** has been raised[14] and was left open until the dynamics of **2** could be handled by computational means. The conformational energy surface of **2** produced here provides some insights into the mechanism of the probable dynamic disorder (see below).

The presence of disorder cannot be excluded. Imagine that the crystal is composed of either a racemic mixture of the D_5 forms, **2a (m–PPPPP)** and **2a' (p–MMMMM)**, or consists of the molecules, each of which equilibrates between the two enantiomeric forms of the global energy minimum. In any case the average picture would be compatible with both D_5 forms being left drawings show two enantiomeric molecules (**2a**, **2a'**) overlapped and the right drawings the same view obtained from the x-ray structure analysis.
obtained from the x-ray structure analysis.

The full graph of the conformational energy surface of **2** is so complex that only a reduced graph (enantiomers are preserved as different species) is given in Figure 8. The thick line on the graph shows the lowest energy pathway connecting the two D_5 global energy minima. All the information (relative free energy, symmetries of the species, lowest vibrational frequencies and helical indices) and relevant conformational features of each stationary point depicted herein are available from the authors.

There are eight deep energy minima on the surface [**2a (m–PPPPP)**, **2e (m–MPPPP)**, **2i (m–MMPPP)**, **2v (m–MPMPP)** and their enantiomers] separated by partial pathways, each of which contains two transition points and one high-energy minimum. Figure 9 shows a simplified interconversion graph wherein only these eight low-energy conformers are depicted. The structures of the unique minima (**2e**, **2i** and **2v**) and the structure of the highest transition state **2l (m–MMXPP)**, 15·6 kcal mol^{-1} higher in free energy

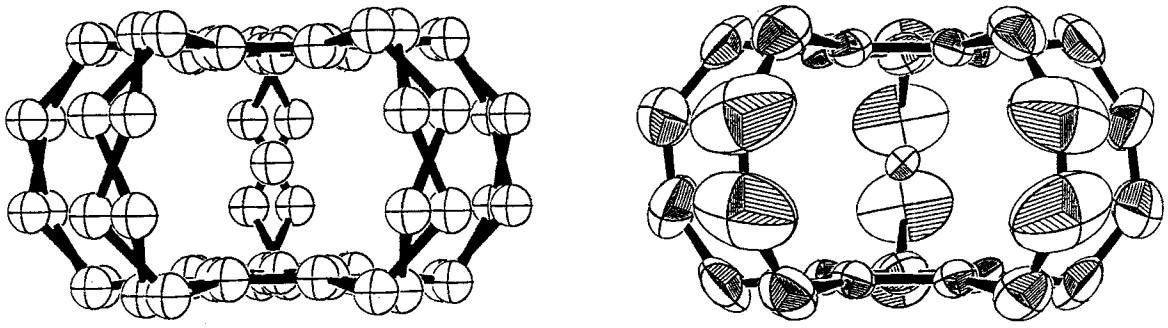

Figure 7. ORTEP drawings (side view) of the overlapped D_5 enantiomers (**2a**, **2a'**) of global energy minimum conformer of [4]superferrocenophane (left drawing) and its structure produced by x-ray analysis (right drawing). See text for explanation

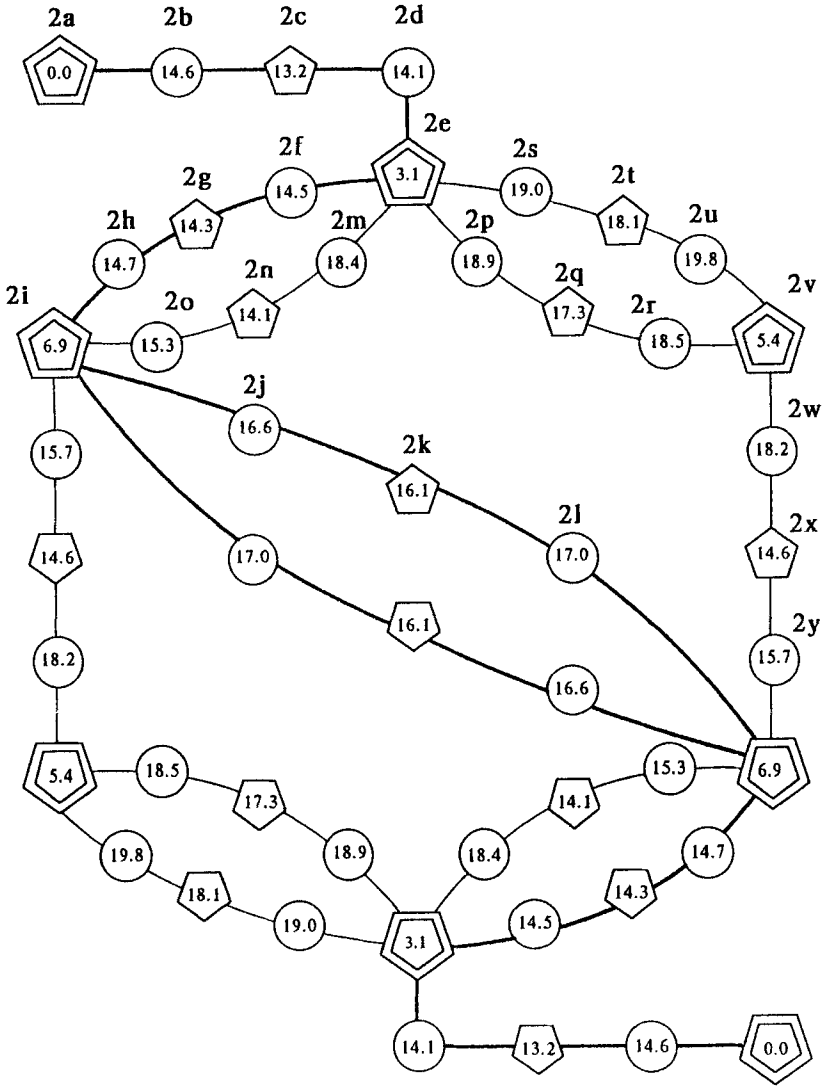

Figure 8. Reduced graph of the MM2′ conformational energy surface of [4]superferrocenophane (**2**). Pentagons and circles denote minima and saddle points, respectively. Deep energy minima are marked by double pentagons. Entries inside pentagons and circles are relative steric energies. The thick line shows the lowest energy path

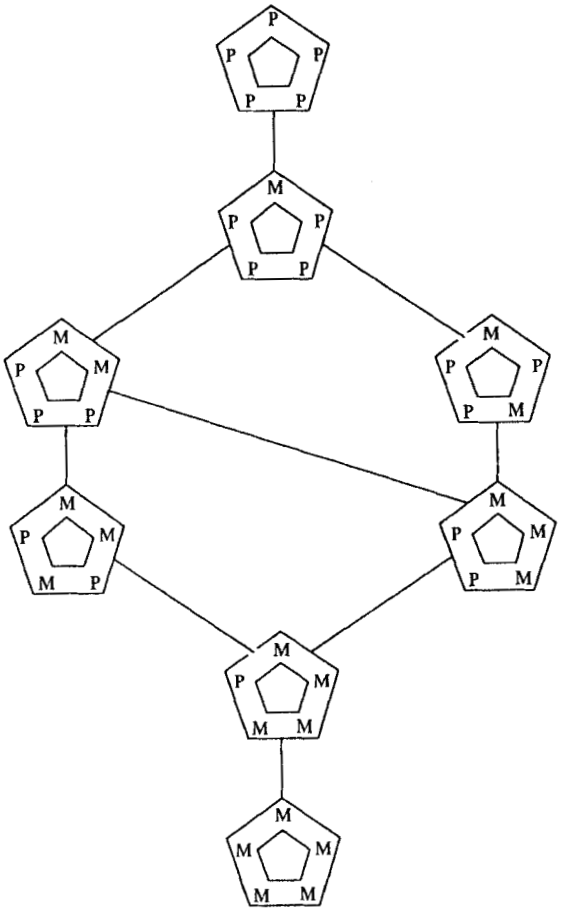

Figure 9. Simplified interconversion graph of [4]superferrocenophane (**2**) (compare with Figure 8). Only deep energy minima are preserved here. **P** and **M** denote the helical sense of the bridges

than **2a**, on the lowest energy path are given in Figure 10.

Among the deep energy minima, apart from the global energy minimum (**2a**), only **2e** (**2e′**) has relatively low potential ($3 \cdot 1$ kcal mol^{-1}) and free ($2 \cdot 3$ kcal mol^{-1}) energies. This conformer is formed when one bridge in **2a** is inverted. It is interesting that the pathway from **2a** through **2e** is simpler than the corresponding one-bridge inversion in [4](1,1′)ferrocenophane (**9**) (compare Figure 4 with Figure 9). There

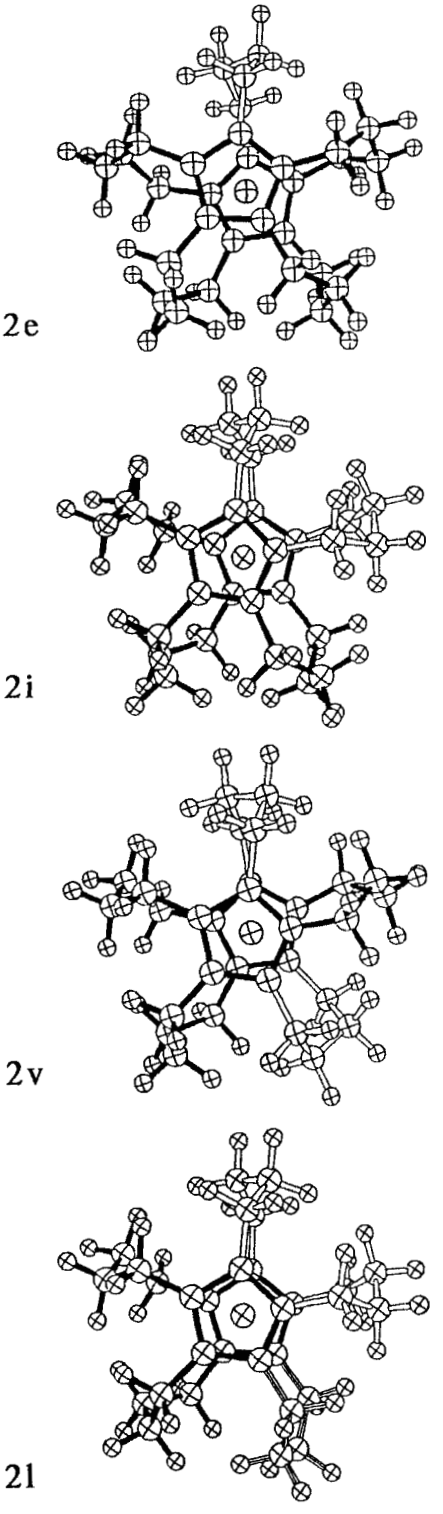

Figure 10. Structures of 'deep' energy minimum conformers (**2e**, **2i** and **2v**) and the highest transition state on the lowest energy path (**2l**) for the inversion of [4]superferrocenophane. Black and white colours of the bridges denote **P** and **M** helicity, respectively. Bonds of the flipping bridge (X) in **2l** are drawn by triple lines

are only three stationary points on the way from **2a** to **2e** whereas there are nine between **9a** and **9a'**. Clearly, the presence of additional bridges in **2** constrains the motion of bridges. Unlike **9**, the relative twist of cyclopentadienyl rings in **2** is strictly concerted with bridge reversal. Further, the presence of five tetramethylene bridges in **2** increases the barrier height of the bridge reversal, hence the molecule is apparently more rigid than **9**: the calculated barrier height of bridge interconversion of **2a** to **2e** costs at least twice as much as that of **9**. Note that the entropy effect related to the degeneracy of the energy surface of **2** contributes substantially to the lowering of the overall energy barrier. The pathway between **2a** and **2e**, for instance, is tenfold degenerate.

The surface represented by a graph in Figure 9 corresponds to the one-by-one bridge flipping process.[48] The stepwise interconversion mechanism seems to be most probable. One-step interconversion via a D_{5h} would-be transition state seems impossible: the calculated energy of the D_{5h} structure is 147 kcal mol^{-1} higher than that of **2a** and it is an 11-dimensional partial maximum.

Although every effort has been made to locate all possible stationary points on the conformational energy surface of **2**, there is no certainty that nothing has been missed. Moreover, one could ask whether the mechanism involving, for instance, two or more bridges flipping together with shifted phase, is not of lower energy than the pathways of the proposed one-by-one bridge flipping mechanism. In fact, this possibility has been considered in the course of the search of the energy surface, but so far has never been found.

CONCLUSION

The purpose of this work was to develop a molecular mechanical model applicable to conformational studies of ferrocenes bridged with hydrocarbon chains, in an extension of our preliminary work[14] on hydrocarbon models. A set of x-ray structures of variously bridged ferrocenes (possessing different numbers and sizes of bridges) was used to fit parameters within the new force field proposed: the iron atom is covalently bonded to all ten cyclopentadienyl carbon atoms, which preserve their aromatic character.

A difficulty arose in differentiating various types of bond angles present in the ferrocene molecule, which involve angles centred on the iron atom and extended to carbon atoms of different cyclopentadienyl rings. This problem was circumvented by modifying the form of bending potential involving these angles: the potential follows the usual Allinger's equation for angles smaller than the equilibrium bond angle in ferrocene itself and vanishes for larger angles. Such a treatment proved sufficient to control the relative tilt motion of the cyclopentadienyl ring planes.

In the present force-field model, the two cyclopentadienyl rings of the ferrocene molecule can rotate almost freely. Geometry optimization results in a staggered conformation, which is a minimum on the potential energy surface. The eclipsed form is a saddle point connecting staggered forms, and the calculated energy barrier to this internal rotation amounts to 0·96 kcal mol^{-1}. The agreement between the calculated and observed salient structural features in the series of ferrocenophanes, which were used to fit the parameters, is good.

The conformational energy surfaces of three ferrocenophenes (**2**, **3** and **9**) have been extensively searched for important stationary points. One- and multidimensional partial maxima are correlated with corresponding energy minima and partial maxima of smaller indices, respectively. The graph–topological approach is applied to describe these conformational energy surfaces. Three kinds of interconversion graphs are used to illustrate hypersurfaces. Energy relationships between the stationary points are described in terms of relative steric and free energies.

These energy surfaces are correlated with available NMR data. In the case of [3]ferrocenophane (**3**), for which variable-temperature studies have been reported, the calculated energy barrier to bridge reversal shows good agreement with the experiment.

In view of our calculations, it is very likely that the global energy minimum conformer of [4]superferrocenophane (**2**) is of D_5 symmetry with all five tetramethylene bridges in an identical helical sense. The bridges can flip one by one over barriers of 13–15 kcal mol^{-1}. The D_{5h} structure, as it appears from x-ray analysis, does not represent a stationary point on the energy surface. The model proposed here can be applied to studies of yet unsynthesized members of this family.

ACKNOWLEDGEMENTS

Thanks are due to Professors Hisatome and Yamakawa for suggesting the problem and participating in many helpful discussions. Partial financial support from the Ministry of Education, Science and Culture, through Grants-in-Aid for Scientific Research (Nos 03554020 and 03214105), is gratefully acknowledged. J. M. R. thanks this Ministry for a graduate fellowship, 1984–89.

REFERENCES

1. T. J. Kealy and P. L. Pauson, *Nature* (London) **168**, 1039 (1966).
2. S. A. Miller, J. A. Tebboth and J. F. Tremaine, *J. Chem. Soc.* 632 (1952).
3. G. B. Kauffman, *J. Chem. Educ.* **60**, 185 (1983).
4. M. Hisatome, J. Watanabe, K. Yamakawa and Y. Iitaka, *J. Am. Chem. Soc.* **108**, 572 (1986).

5. M. Hisatome, J. Watanabe, K. Yamakawa, K. Kozawa and T. Uchida, *J. Organomet. Chem.* **262**, 365 (1984).
6. T. H. Barr and W. E. Watts, *Tetrahedron* **24**, 6111 (1968).
7. M. Hisatome, J. Watanabe, Y. Kawarjiri, K. Yamakawa and Y. Iitaka, *Organometallics* **9**, 497 (1990).
8. M. Marsili, *Computer Chemistry*, Chapt. 4. CRC Press, Boca Raton, FL (1989).
9. D. M. Hirst, *A Computational Approach to Chemistry*, Chapt. 3. Blackwell, Oxford (1990).
10. S. Wilson, *Chemistry by Computer*, Chapt. 5. Plenum Press, New York (1986).
11. T. Clark, *A Handbook of Computational Chemistry*, Wiley, New York (1985).
12. U. Burkert and N. L. Allinger, *Molecular Mechanics*, American Chemical Society, Washington, DC (1982).
13. K. Rasmussen, *Potential Energy Functions in Conformational Analysis*, Springer, Berlin (1985).
14. J. M. Rudziński, E. Ōsawa, M. Hisatome, J. Watanabe and K. Yamakawa, *J. Phys. Org. Chem.* **2**, 602 (1989).
15. J. C. A. Boeyens and D. C. Levendis, *S. Afr. J. Chem.* **35**, 144 (1982).
16. F. M. Menger and M. J. Sherrod, *J. Am. Chem. Soc.* **110**, 8606 (1988).
17. H.-J. Thiem, M. Brandl and R. Breslow, *J. Am. Chem. Soc.* **110**, 8612 (1988).
18. A. J. Campbell, C. A. Fyfe, D. Harold-Smith and K. R. Jeffrey, *Mol. Cryst. Liq. Cryst.* **30**, 1 (1976).
19. V. S. Allured, C. M. Kelly and C. R. Landis, *J. Am. Chem. Soc.* **113**, 1 (1991).
20. R. B. Nachbar, Jr and K. Mislow, *QCPE* No. 514.
21. *Japan Chemistry Program Exchange* to be submitted.
22. R. B. Nachbar, Jr, W. D. Hounshell, V. A. Naman, O. Wennerström, A. Guenzi and K. Mislow, *J. Org. Chem.* **48**, 1227 (1983).
23. H.-B. Bürgi, W. D. Hounshell, R. B. Nachbar, Jr, and K. Mislow, *J. Am. Chem. Soc.* **105**, 1427 (1983).
24. R. B. Nachbar, Jr. and K. Mislow, attached to QCPE program, ref. 20. *BIGSTRN3 Program Instruction Manual*, and references cited therein.
25. O. Ermer, *Aspekte von Kraftfeldrechnungen*, Wolfgang Baur, Munich (1981).
26. C. Jaime and E. Ōsawa, *Tetrahedron* **39**, 2769 (1983).
27. Z. Slanina, *Contemporary Theory of Chemical Isomerism*, Academia, Prague (1986).
28. P. G. Mezey, *Potential Energy Hypersurfaces, Studies in Physical and Theoretical Chemistry*, Vol. 53. Elsevier, Amsterdam (1985).
29. N. L. Allinger and Y. H. Yuh, *Operating Manual of MM2 Program, QCPE* No. 395.
30. I. Hyams, *J. Chem. Phys. Lett.* **15**, 88 (1972).
31. B. E. Douglas, D. H. McDaniel and J. J. Alexander, *Concepts and Models of Inorganic Chemistry*, p. 77. Wiley, New York (1983).
32. A. L. Allred, *J. Inorg. Nucl. Chem.* **17**, 215 (1961).
33. N. L. Allinger, *J. Am. Chem. Soc.* **99**, 8127 (1977).
34. A. Haaland and J. E. Nilsson, *Acta Chem. Scand.* **22**, 2653 (1968).
35. M. Hillman and J. D. Austin, *Organometallics* **6**, 1737 (1986).
36. M. B. Laing and K. N. Trueblood, *Acta Crystallogr.* **19**, 373 (1965).
37. M. Hisatome, Y. Kawajiri and K. Yamakawa, *J. Organomet. Chem.* **236**, 359 (1982).
38. M. Hisatome, J. Watanabe, K. Yamakawa, K. Kozawa and T. Uchida, *Nippon Kagaku Kaishi*, 572 (1985).
39. F. Tokusagawa and T. F. Koetzle, *Acta Crystallogr., Sect. B*, **35**, 1074 (1979).
40. P. Seiler and J. D. Dunitz, *Acta Crystallogr., Sect. B*, **35**, 1068, 2020 (1979), **38**, 1741 (1982).
41. F. Calvarin, J. F. Berar and G. Clec'h, *J. Phys. Chem. Solids*, **43**, 785 (1982).
42. E. W. Abel, M. Booth and K. G. Orrell, *J. Organomet. Chem.* **208**, 213 (1981).
43. M. Rosenblum, A. K. Banerjee, N. Danieli, R. W. Fish and V. Schlatter, *J. Am. Chem. Soc.* **85**, 316 (1963).
44. E. W. Abel, M. Booth, C. A. Brown, K. G. Orrell and R. L. Woodford, *J. Organomet. Chem.* **214**, 93 (1981).
45. A. Lüttringhaus and W. Kullick, *Angew. Chem.* **70**, 438 (1958).
46. H. Lumbroso, C. Pigenet, H. L. Lentzner and W. E. Watts, *Tetrahedron* **28**, 111 (1972).
47. T. S. Cameron and R. E. Cordes, *Acta Crystallogr., Sect. B*, **35**, 748 (1979).
48. E. Ōsawa, *J. Am. Chem. Soc.* **101**, 5523 (1979).